Diffusivities of Lysozyme in Aqueous $MgCl_2$ Solutions from Dynamic Light-Scattering Data: Effect of Protein and Salt Concentrations

J. J. Grigsby,[†] H. W. Blanch,[†] and J. M. Prausnitz*[,†,‡]

Chemical Engineering Department, University of California, Berkeley, California 94720, and Chemical Sciences Division, Lawrence Berkeley Laboratory, Berkeley, California 94720

Received: September 9, 1999; In Final Form: December 20, 1999

Dynamic light-scattering (DLS) studies are reported for lysozyme in aqueous magnesium chloride solutions at ionic strengths 0.6, 0.8, and 1.0 M for a temperature range 10−30 °C at pH 4.0. The diffusion coefficient of lysozyme was calculated as a function of protein concentration, salt concentration, temperature, and scattering angle. A Zimm-plot analysis provided the infinitely-dilute diffusion coefficient and the protein-concentration dependence of the diffusion coefficient. The hydrodynamic radius of a lysozyme monomer was obtained from the Stokes−Einstein equation; it is 18.6 ± 1.0 Å. The difference (1.4 Å) between the hydrodynamic and the crystal-structure radius is attributed to binding of Mg^{2+} ions to the protein surface and subsequent water structuring. The effect of protein concentration on the diffusion coefficient indicates that attractive interactions increase as the temperature falls at fixed salt concentration. However, when plotted against ionic strength, attractive interactions exhibit a maximum at ionic strength 0.84 M, probably because Mg^{2+}−protein binding and water structuring become increasingly important as the concentration of magnesium ion rises. The present work suggests that inclusion of ion binding and water structuring at the protein surface in a pair-potential model is needed to achieve accurate predictions of protein-solution phase behavior.

Introduction

Salt-induced protein precipitation from aqueous solution is often the sole step in protein purification when crude fractionations of protein are sufficient, or provides a first step when the protein is subsequently further purified by other methods such as chromatography or electrophoresis.[1,2] No useful theoretical model is now available to predict solution conditions that induce the selective precipitation of a target protein. The initial step for developing a predictive molecular-thermodynamic model is to quantify the effect of solution conditions on intermolecular forces between protein molecules.

Understanding intermolecular forces between protein molecules is also vital for protein-crystallization science and technology. High-quality crystals are necessary for determining three-dimensional protein structure by X-ray crystallography. Finding conditions that yield high-quality crystals is often the most time-consuming step in the structure-determination process.

Recent work has focused on correlating precipitation and crystallization conditions with the osmotic second virial coefficient and the potential of mean force (PMF).[3−8] Dynamic light scattering (DLS) data give the dependence of the protein diffusion coefficient on the protein concentration and solution conditions. This dependence can be related to the PMF to obtain model parameters.[9,10] Once a model for the PMF is available, the second osmotic virial coefficient can be calculated.[11] George and Wilson have shown that the crystallization of lysozyme occurs over a narrow range of second virial coefficient values.[4] For positive coefficients (i.e., repulsive interactions) lysozyme remains stable in solution, but when the coefficient is large and negative, lysozyme forms an amorphous precipitate.

Hen egg white lysozyme has been extensively studied due to its compact globular structure and stability over a wide range of solution conditions. Sophianopoulos and Van Holde were the first to report the pH-dependent self-association of lysozyme.[12,13] Equilibrium-sedimentation studies revealed lysozyme aggregation at 20 °C in 0.15 M KCl solutions for protein concentrations up to 15 g/L. Later studies showed that the pH-dependent dimerization mechanism involved the deprotonated form of Glu-35 in the active site (Glu-35 has an unusually high pK_a of 6.3).[14] Below pH 4.5, there is no dimerization because the Glu-35 carboxylic acid remains protonated. Lysozyme aggregation is a result of the attractive interaction between the deprotonated Glu-35 carboxylic acid and a protonated nitrogen on the Trp-62 side chain of a neighboring lysozyme molecule. This leads to a head-to-tail association.[15−18]

In this work, DLS measurements are reported for hen egg white lysozyme at concentrations to 30 g/L in aqueous $MgCl_2$ solutions for the temperature range 10−30 °C. Solution pH was maintained at pH 4.0 to ensure that any lysozyme association is not due to head-to-tail association. Kuehner et al. have performed DLS experiments with lysozyme in aqueous ammonium-sulfate solutions for an ionic strength range 0.05−5 M and pH range 4.0−7.0.[9] Ammonium sulfate preferentially hydrates the lysozyme surface.[19] $MgCl_2$ was chosen for this study because Mg^{2+} is a highly kosmotropic ion that is able to bind to protein surfaces and to structure water.[20]

Materials and Methods

Lysozyme Solution Preparation. Lysozyme was purchased from Boehringer Mannheim (Germany). Pusey et al. have shown that the solubility and quality of protein crystals achieved is dependent on the purity and nature of the starting materials.[21] Gel electrophoresis showed less than 1% contamination by other proteins, and therefore no further purification was performed. Reagent-grade $MgCl_2$ was purchased from Fischer Scientific

[†] University of California.
[‡] Lawrence Berkeley National Laboratory.

10.1021/jp993177s CCC: $19.00
Published on Web 03/25/2000

(Pittsburgh, PA). Syringe-tip 0.2 μm poresize filters were purchased from Millipore (Bedford, MA). Deionized water was obtained from a Barnstead-Nanopure II filtration unit.

A 4 L stock solution of salt was prepared by weighing the appropriate amount of salt for a given ionic strength and dissolving it in deionized water. The pH of the solution was adjusted to 4.0 using aqueous HCl of the same ionic strength as that of the salt solution. Lysozyme was dissolved in 20 mL of the salt-stock solution. Although gel electrophoresis showed minimal protein contaminants, small amounts of salts are present in the lyophilized lysozyme. While these salts are not significant scattering species compared to lysozyme, they may influence protein−protein interactions. Therefore, the protein−salt solution was dialyzed against the salt solution to minimize the amount of salt contaminants. Dialysis tubing with a molecular-weight cutoff of 6000−8000 was purchased from Spectrum Medical Industries (Los Angeles, CA). After dialysis, the pH of the protein−salt solution was adjusted with HCl of the same ionic strength as that of the salt-stock solution. Since the protein solution has a small natural buffering capacity, the pH was stable over the duration of the light-scattering measurements. The pH of the solution was measured after each series of measurements to check pH stability.

Precision-ground Pyrex NMR tubes with 12 mm o.d., 0.5 mm wall thickness (Wilmad Glass, Buena, NJ), and 5 mL volume were thoroughly cleaned before sample loading. The tubes were stored in concentrated H_2SO_4 until needed. They were first rinsed with filtered deionized water and placed in a 2 M NaOH solution containing 3.5 g/L $KMnO_4$ for 2 h. The tubes were again rinsed with filtered deionized water and stored in 1 M HCl until needed. Before sample loading, the tubes were again rinsed with filtered deionized water and allowed to dry. All transfers were performed in a laminar-flow hood to minimize dust contamination.

A tube-cap assembly permitted the closed-loop filtration of the protein−salt solution. This design was essential for the removal of small aggregates of protein and dust which are significant light scatterers. The tubing was connected to a syringe containing the sample solution and rinsed with the solution. The tube-cap assembly was next connected to the sample tube and filled with the protein−salt solution. The closed-loop system contained a 0.2 μm filter to facilitate the continuous filtration of the sample. Samples were filtered using a peristaltic pump for a minimum of 30 min at the lowest setting of the pump to prevent shear denaturation of the protein.

Dynamic Light-Scattering Measurements. The DLS system contains an Innova-90 argon ion laser (Coherent Inc., Santa Clara, CA), tuned to a wavelength of 488 nm, a BI-240SM multiangle goniometer, a BI-EMI-9865 photomultiplier, and a BI-9000 digital autocorrelator. The autocorrelator is able to measure the electric-field autocorrelation function, $g^E(\tau)$, in real time allowing for the calculation of *z*-average diffusion coefficients. Decalin (Aldrich 29477-2, CAS [91-17-8], refractive index $n = 1.47$) was used as an index-matching liquid to reduce flare at the glass−liquid interface. The decalin was recirculated through a 47 mm OD 0.1 μm pore size hydrophobic membrane filter (GSEP 047A0, Millipore) until all visible dust was removed. The sample in the light-scattering apparatus was allowed to equilibrate thermally for at least 1 h. Constant temperature was achieved with a VWR model 1160 recirculating water bath.

Dynamic light-scattering (DLS) measurements were made for a range of scattering angles at 10° increments from 30° to 90°. The range covered by the correlation function for each angle was determined before measurements were taken. No obvious humps or long tails were observed in the correlation function that would indicate protein aggregation for the duration of the experiment. At least three measurements were made at each angle. Time for data collection ranged from 10 min to 1 h depending on the protein concentration and the angle of detection. A minimum of 5×10^8 photons was collected for statistically meaningful data. Data were rejected if the difference between the calculated and measured baselines was greater than 0.02%. The data was time-independent over the course of a run, typically 6 h. To ensure that thermal equilibrium was maintained throughout the duration of the experiment, an additional measurement at 30° was taken and compared to the 30° measurements at the start of the experiment. No significant differences were observed.

The temperature was lowered by 5 °C after each series of measurements. Again the sample was allowed to equilibrate for at least 1 h before measurements were made. The temperature of the sample was not lowered below 10 °C due to fogging of the windows on the light-scattering apparatus. Light-scattering measurements were made for a specific ionic strength and temperature at three protein concentrations.

The pH of the sample solution was checked after each series of measurements. For any experiment, the change in pH was less than 0.1 units. The filtration process removed aggregates of lysozyme. The concentration of lysozyme generally decreased no more than 5% from the initial concentration. Protein concentrations were determined by measuring absorbance at 280 nm and 25 °C using a Beckman DU-6 spectrophotometer with an extinction coefficient for lysozyme of 2.635 L/(g cm).[22] The refractive index of the protein solution was measured at the appropriate temperature using a Zeiss refractometer and white light. Refractive indices increased linearly with protein concentration with a refractive index increment of 0.18 mL/g. This is a typical value for most proteins. Viscosity of $MgCl_2$ solutions as a function of ionic strength and temperature was measured using an Ubbelohde viscometer with water as a reference.

Data Reduction. DLS measurements were made at three protein concentrations for an ionic strength (IS) range of 0.6−1.0 mol/L and a temperature range of 10−30 °C. Measurements could not be obtained for IS 1.0 mol/L at 10 and 15 °C due to the appearance of crystals within the time frame of DLS measurements. No appearance of crystals was detected for the other salt and protein concentrations within the time frame of the measurements.

The signal generated by the light scattered from diffusing particles can be analyzed by its intensity autocorrelation function, $G^I(\tau)$:

$$G^I(\tau) = \langle I(t) \cdot I(t + \tau) \rangle \tag{1}$$

where $I(t)$ is the scattered-light intensity at time t and $I(t + \tau)$ is the scattered-light intensity at some later time $(t + \tau)$. The normalized intensity autocorrelation function $g^I(\tau)$ is

$$g^I(\tau) = \frac{G^I}{\langle I(t) \rangle^2} \tag{2}$$

The electric-field autocorrelation function, $g^E(\tau)$, is related to the normalized intensity autocorrelation function by

$$g^I(\tau) = 1 + B[g^E(\tau)]^2 \tag{3}$$

where B is an equipment parameter.

For a monodisperse system of particles, $g^E(\tau)$ follows a simple exponential decay with decay constant Γ.

$$g^E(\tau) = \exp[-\Gamma\tau] \tag{4}$$

For a system containing a distribution of different-sized particles, $g^E(\tau)$ becomes the sum of the electric-field autocorrelation functions of each of the species weighted by the concentration of the species in solution. The quadratic cumulant expansion analysis was used to obtain an apparent decay constant, Γ_{ap}, which represents an average decay constant for all species in solution (monomers, dimers, ect.).[23] The second cumulant in the analysis, Q, provides an indication of the polydispersity of the system. For most experiments, Q was less than 0.02, indicating a narrow protein-size distribution with few aggregates. For the few cases when Q was greater than 0.02, inversion of the autocorrelation function was performed with a Brookhaven Instruments Corp. version of CONTIN program.[24,25] CONTIN results showed a narrow unimodal diffusion-coefficient distribution near the value given by the quadratic-cumulant result. This analysis showed that lysozyme is a monomer at solution conditions studied here.

The apparent diffusion coefficient, D_{ap}, for lysozyme molecules was calculated from

$$D_{ap} = \frac{\Gamma_{ap}}{q^2} \tag{5}$$

where q is the magnitude of the scattering vector. An apparent diffusion coefficient is used here since Γ_{ap} is an intensity-weighted concentration average of all species (monomers, dimers, etc.) in the aqueous protein solution. The magnitude of the scattering vector was calculated from

$$q = \frac{4\pi n}{\lambda_{laser}} \sin(\theta/2) \tag{6}$$

where n is the refractive index of the protein salt solution, λ_{laser} is the wavelength of the laser light, and θ is the scattering angle of detection. The difference in the D_{ap} values at a specific salt and protein concentration for a given scattering angle was always less than 4%. This difference was random and did not increase or decrease with time.

A Zimm plot was constructed for each ionic strength and temperature. Diffusion coefficients are plotted as a function of both concentration and angle. D_{ap} was plotted for each protein concentration as a function of $q^2 + kc_p$, which depends both on the scattering angle [$q \approx \sin(\theta/2)$] and protein concentration c_p. The parameter k is chosen to facilitate graphical inspection of the Zimm plot; the value of k does not affect the results. Figure 1 shows a representative Zimm plot for $MgCl_2$ ionic strength 0.80 M at 25 °C. At constant protein concentration, the open symbols represent the diffusion coefficient extrapolated to zero angle. At constant angle, the open symbols represent the diffusion coefficient extrapolated to zero protein concentration. The two extrapolated lines intersect at a point D_o, that represents the diffusion coefficient of a lysozyme molecule in an infinitely-dilute protein solution. Table 1 summarized the calculated values of D_o. The measured values of D_{ap} showed little dependence on the magnitude of the scattering vector, q, indicating monodisperse samples. Several authors have reported the diffusion coefficient of lysozyme in bulk solution to be $(8-10) \times 10^{-7}$ cm^2/s at temperatures of 20−25 °C.[10,26,27] Since the diffusion coefficient depends on temperature, salt concentration, and protein concentration, our results agree well with these previous studies.

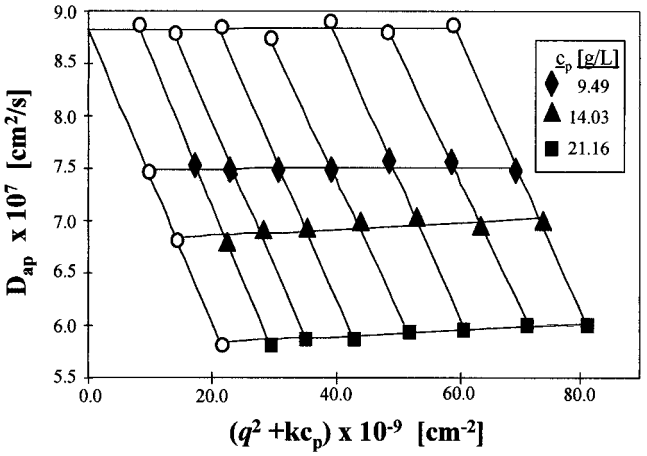

Figure 1. Zimm plot. Dependence of the apparent diffusion coefficient of lysozyme on protein concentration and scattering angle for a $MgCl_2$ solution at IS 0.80 M, pH 4.0, and 10 °C.

TABLE 1: Zero-Angle Apparent Diffusion Coefficients of Lysozyme as a Function of Temperature and Ionic Strength of $MgCl_2$

T (°C)	$10^7 D^o_{ap}$ (cm^2/s)	T (°C)	$10^7 D^o_{ap}$ (cm^2/s)	T (°C)	$10^7 D^o_{ap}$ (cm^2/s)
Ionic Strength 1.00 M		Ionic Strength 0.80 M		Ionic Strength 0.60 M	
20	10.6	10	8.79	10	8.32
25	11.5	15	9.97	15	9.40
30	12.2	20	11.4	20	10.5
25	12.9	25	11.6		
		30	14.1	30	13.0

Infinite-Dilution Hydrodynamic Radii. The crystal structure of hen egg white lysozyme determined by X-ray crystallography (Brookhaven protein database structure 2LYZ) is a prolate ellipsoid of revolution with major semiaxis $\alpha_x = 22.5$ Å and symmetric minor semiaxes $\beta_x = 15$ Å. Because of the compact nature of lysozyme and rapid rotational tumbling in solution, lysozyme can be considered to be roughly spherical in shape. The equivalent spherical radius of a lysozyme monomer is 17.2 Å.

The infinite-dilution hydrodynamic radius, r_H, is calculated from the Stokes−Einstein equation for infinitely dilute monodisperse spheres:

$$D_o = \frac{k_B T}{f_o} = \frac{k_B T}{6\pi\eta_o r_H} \tag{7}$$

where f_o is the hydrodynamic friction factor, k_B is Boltzmann's constant, T is absolute temperature, and η_o is the viscosity of the solvent. Values for η_o were determined from viscosity measurements. A comparison plot of the calculated hydrodynamic radii of lysozyme in $MgCl_2$ solutions is given in Figure 2. The difference between the calculated hydrodynamic radius and the crystal structure radius is 1.4 Å. This difference is attributed to possible ion binding and hydration at the protein surface. There does not appear to be a clear trend for the hydrodynamic radius as a function of ionic strength or temperature. The average hydrodynamic radius from the DLS data is 18.6 ± 1 Å.

Kuehner et al. performed similar DLS studies with lysozyme in ammonium sulfate solution and calculated a hydration-layer thickness of 0.8 Å.[9] Nicoli and Benedek reported a hydrodynamic radius of 18.5 Å from DLS measurements over a pH range of 1.2−2.3 in solutions of 0.2 M potassium chloride.[28] Muschol and Rosenberger found a hydrodynamic radius of 19 Å for lysozyme in sodium chloride and acetate solutions up to

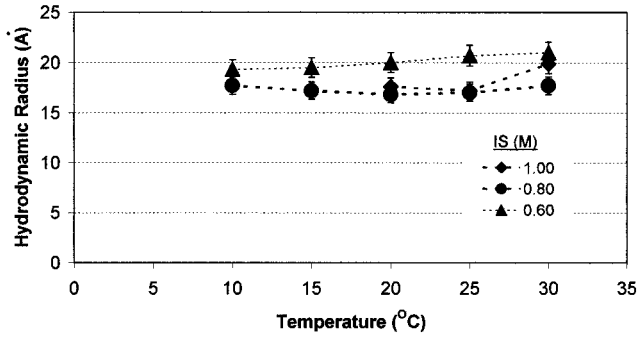

Figure 2. Hydrodynamic radius of lysozyme in $MgCl_2$ solutions at various ionic strengths.

0.5 M at pH 4.7.[29] Skouri et al. reported a hydrodynamic radius of 22 Å in sodium chloride solutions at pH 4.6 over a temperature range of 13−22 °C.[30] Differences in the literature values for the hydrodynamic radius of lysozyme may be due to differences in salt type and concentration, and experimental techniques.

One clear observation of the various DLS studies of lysozyme in salt solutions is that the measured hydrodynamic radius is always greater than the radius found from the crystal structure. Water molecules are bound to the surface of the protein and diffuse with the protein. Roughly 0.3 g of water is bound for every gram of protein. At the surface of the protein, salt ions may bind tightly due to specific salt−protein interactions within the Stern layer, or associate more loosely within the Gouy−Chapman layer. The hydration of the protein surface and ion binding affect the measured diffusivities. The ion effects depend strongly on salt type and concentration and, to a lesser degree, on pH.[31,32] One method to determine the extent of ion binding as a function of salt concentration would be to perform NMR relaxation experiments.

Concentration-Dependent Diffusivities. Figure 3(a−c) shows the normalized apparent diffusion coefficient D^o_{ap}/D_o plotted as a function of protein volume fraction at fixed ionic strength, where D^o_{ap} is the zero-angle extrapolated value at each protein concentration. Protein concentration is expressed in terms of protein volume fraction given by $\phi = c_p M\nu/1000$, where M is the molecular weight of lysozyme (14 400 g/mol) and ν is the partial specific volume of lysozyme (0.703 mL/g).[13] The slope of this line termed the interaction parameter, λ, contains information about interactions between protein molecules. The dependence of λ on protein concentration can be written as

$$D^o_{ap} = D_o(1 + \lambda\phi + O(\phi^2) \qquad (8)$$

where $O(\phi^2)$ indicates higher order terms. The dependence of D^o_{ap}/D_o on volume fraction was linear for all data.

Pusey and Tough give an excellent review of the theoretic work regarding particle interactions in solution.[33] Theoretical expressions have been derived for λ to account for hydrodynamic and interparticle interactions. Hydrodynamic interactions arise from the influence of the fluid-flow field of a diffusing particle on another diffusing particle. Interparticle interactions include Coulombic, van der Waals, and other specific forces. As the attractive interactions between diffusing particles increases, the rate of diffusion decreases. Relationships between λ and the potential of mean force (PMF) have been derived for monodisperse systems.[34−38] Negative values of λ indicate a net attractive interaction and positive values indicate a net repulsive interaction. Figure 3(a−c) shows that λ becomes more negative as temperature decreases at fixed ionic strength, indicating increasing attractive interactions, as expected.

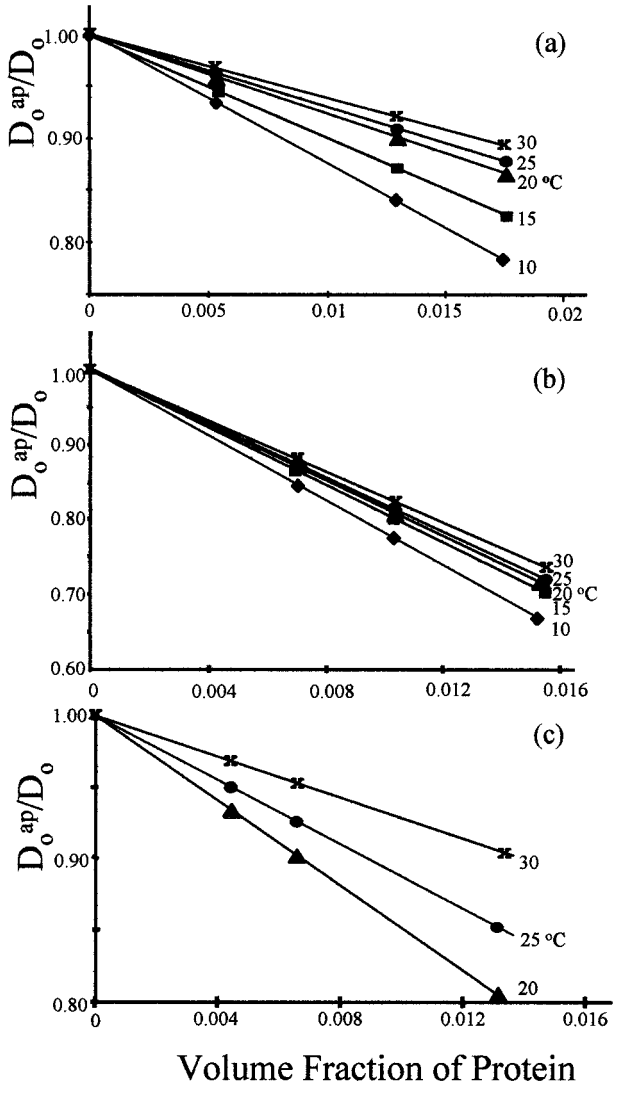

Figure 3. Determination of the interaction parameter, λ, for aqueous lysozyme in $MgCl_2$ solutions at pH 4.0 and ionic strength (a) 0.60, (b) 0.80, and (c) 1.00 M. λ is the slope of the lines shown here.

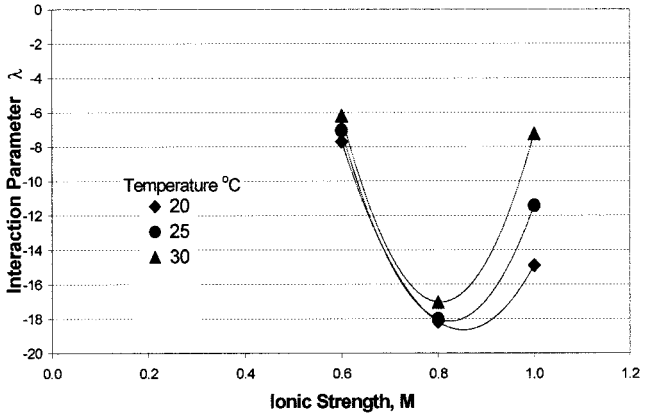

Figure 4. Interaction parameter λ as a function of $MgCl_2$ ionic strength at different temperatures.

Figure 4 shows λ as a function of volume fraction of protein at fixed temperature. The interaction parameter attains a minimum near ionic strength 0.80 M indicating maximum attraction. This observation is unexpected because previous studies with lysozyme in other salt-solution systems have shown λ to decrease monotonically as salt concentration rises.[9−10,27]

The previous studies contained salts that preferentially hydrate the lysozyme surface.

Arkawa et al. performed densimetry experiments with lysozyme in $MgCl_2$ solutions at pH 3.0 and 4.5 and found preferential binding of Mg^{2+} to the surface of the protein.[19] On the basis of their results, 5−6 Mg^{2+} ions are estimated to bind to the lysozyme surface for conditions used in this study. Mg^{2+} is a highly kosmotropic ion that structures water around the ion.[20] Therefore, the binding of Mg^{2+} to the lysozyme surface structures water around the protein molecule, adding a hydration layer of 1.4 Å.

Arakawa et al. determined the solubility of lysozyme in $MgCl_2$ solutions. The solubility near zero salt concentration is very high (>250 g/L) and sharply decreases to a minimum solubility at ionic strength 0.9 M.[19] Above this salt concentration, the solubility of lysozyme in $MgCl_2$ solutions increases. Our observed minimum in λ at 0.84 M is in very good agreement with Arakawa's solubility studies.

Cloud point temperature (CPT) studies have been reported for lysozyme at a fixed protein concentration 87 g/L in $MgCl_2$ solution at pH 7.8.[39] The CPT is the temperature for liquid−liquid-phase separation. The CPT is an indication of the net attractive interactions between protein molecules; the higher the CPT, the greater the net attractive interactions. Broide reported a maximum in the CPT for lysozyme in $MgCl_2$ solutions at ionic strength 0.9 M. Above $MgCl_2$ ionic strength 0.9 M, the net attractive interactions decrease. Broide's observation is in good agreement with the present study.

Discussion

Numerous authors have described phase behavior of simple colloidal systems using simple pair potentials.[40−42] Several forms of the pair potential have been proposed to represent the strength and range of interactions between protein molecules. Examples of such pair potentials include charge−charge, van der Waals, osmotic, solvation/hydration, and specific interactions. Protein molecules are often represented as hard spheres with uniform charge distribution contained in a continuous saline medium; i.e., the discrete nature of ions is not taken into account when the presence of salt is represented by point charges.

Regression of model parameters for pair potentials has been performed for DLS measurements of lysozyme. Kuehner et al. reported DLS measurements of lysozyme in ammonium sulfate solutions as a function of ionic strength, protein concentration, and pH.[9] The attractive interaction parameter decreases as ionic strength rises but becomes nearly constant at 1.0 M ionic strength due to screening of electrostatic repulsion between proteins molecules. The attractive interaction parameter increases at higher ionic strength due to osmotic attraction of protein molecules at higher salt concentrations. The Hamaker constant and net charge on the protein molecule regressed from DLS data were $8.9k_BT$ and 5.5, respectively. A similar analysis was performed by Eberstein et al. for lysozyme in acetate-buffered (pH 4.2) solutions of sodium chloride at 25 °C.[10] Muschol and Rosenberger performed static and dynamic light-scattering measurements on lysozyme in solutions of sodium chloride and sodium acetate at pH 4.7.[29] The Hamaker constant and protein charge were $7.2k_BT$ and 5.4, respectively.

Pair-potential models are able to qualitatively describe the salting-out of proteins at high salt concentrations. However, at present, no pair potential model is able to account for the present DLS observations, solubility measurements, and CPT results. The models proposed by previous authors cannot explain the salting-in of lysozyme at high $MgCl_2$ concentrations.

Arakawa et al. have shown that, as the concentration of $MgCl_2$ increases, there is a greater extent of Mg^{2+} binding to the surface of lysozyme, bovine serum albumin, and β-lactoglobulin.[19] The extent of Mg^{2+} binding increases as the pH of the solution approaches the isoelectric point because the net positive charge on the protein surface approaches zero. The highly kosmotropic Mg^{2+} ion structures water around itself and consequently produces water structuring around the protein suface.

The Cl^- ion may also bind to the protein surface. Cl^- is a slightly chaotropic.[20] Addition of Cl^- to a solution decreases the water structure of the solution. Although Cl^- may bind to the positively charged sites of the protein surface, this interaction is relatively weak compared to the Mg^{2+}−protein interaction. Therefore, it is likely that the minimum in λ is a consequence of Mg^{2+} binding to the protein surface and not Cl^- binding.

These qualitative comments are supported by our recent CPT data (not published) for lysozyme in several magnesium salt solutions. In these studies, the CPT maximum decreases for magnesium salts as the anion becomes more kosmotropic. The highest CPT maximum was observed for magnesium nitrate. The NO_3^- ion is highly chaotropic and therefore breaks the water structuring around the protein surface. The lowest CPT maximum was observed for magnesium sulfate. The SO_4^{2-} ion is kosmotropic and further increases water structuring around the protein surface. It appears that structuring water around the protein surface plays a critical role in the net attractive force between protein molecules in aqueous solution.

In a similar manner, the minimum observed for λ may be explained by ion binding. At $MgCl_2$ concentrations below the minimum, the addition of salt screens the repulsive interactions between lysozyme molecules and, therefore, there is a greater net attraction between the protein molecules. However, as the concentration of $MgCl_2$ increases, there is a greater extent of Mg^{2+} binding to the protein surface producing more water structuring around the protein molecules. The increased intermolecular repulsion due to solvation of the protein surface is a well-accepted phenomena.[43,44] For protein molecules to come to close approach, the water structure around the protein must be broken. Therefore, as Mg^{2+} concentration increases, structuring of water increases, leading to a greater repulsive barrier and decreased net attractive interaction.

DLVO theory is able to described protein-phase behavior for dilute protein and salt concentrations but not for conditions that typify protein precipitation and crystallization. The current DLS study coupled with solubility and CPT data suggests that the pair-potential models must be modified. A model describing phase behavior must account for interactions beyond Coulombic, van der Waals, and osmotic forces. The extent of ion binding and water structuring at the protein surface and solution must be taken into account. Inclusion of ion binding may explain the effect of different salts on the observed phase behavior of aqueous protein solutions. Also, the pH dependence of the phase behavior may be better understood if the extent of ion binding is known. The pH of the solution determines the net charge on the protein surface, and therefore the extent of ion binding. By taking into account ion binding and water structuring around the protein surface, a better pair-potential model is more likely to predict accurately the qualitative and quantitative nature of protein-solution phase behavior.

Acknowledgment. This work was supported by the National Science Foundation and by the Director, Office of Science, Office of Basic Energy Sciences, Chemical Sciences Division

of the U.S. Department of Energy under Contract DE-AC0376SF0009.

References and Notes

(1) Rothstein, F. P*rotein Purification Process Engineering*, 1st ed.; Dekker: New York, 1994.
(2) Scopes, R. K. *Protein Purification: Principles and Practice*, 3rd ed.; Springer-Verlag: New York, 1994.
(3) Vlachy, V.; Blanch, H. W.; Prausnitz, J. M. *AIChE J.* **1993**, *39*, 215.
(4) George, A.; Wilson, W. W. *Acta Crystallogr. D* **1994**, *50*, 361.
(5) Chiew, Y. C.; Kuehner, D. E.; Blanch, H. W.; Prausnitz, J. M. *AIChE J.* **1995**, *41*, 2150.
(6) Rosenbaum, D.; Zamora, P. C.; Zukoski, C. F. *Phys. Rev. Lett.* **1996**, *76*, 150.
(7) Guo, B.; Kao, S.; McDonald, H.; Asanov, A.; Combs, L.; Wilson, W. W. *J. Crystal Growth* **1999**, *196*, 424.
(8) Neal, B. L.; Asthagiri, D.; Velev, O. D.; Lenhoff, A. M.; Kaler, E. W. *J. Crystal Growth* **1999**, *196*, 377.
(9) Kuehner, D. E.; Hayer, C.; Ramsch, C.; Fornefeld, U. M.; Blanch, H. W.; Prausnitz, J. M. *Biophys. J.* **1997**, *73*, 3211.
(10) Eberstein, W.; Georgalis, Y.; Saenger. W. *J. Crystal Growth* **1994**, *143*, 71.
(11) McMillan, W. G.; Mayer, J. E. *J. Chem. Phys.* **1945**, *13*, 276.
(12) Sophianopoulos, A. J.; Van Holde, K. E. *J. Biol. Chem.* **1961**, *236*, 82.
(13) Sophianopoulos, A. J.; Rhodes, C. K.; Holcomb, D. N.; Van Holde, K. E. *J. Biol. Chem.* **1962**, *237*, 1107.
(14) Sophianopoulos, A. J. *J. Biol. Chem.* **1969**, *244*, 3188.
(15) Blake, C. C. F.; Mair, G. A.; North, A. C. T.; Phillips, D. C.; Sarma, V. R. *Proc. R. Soc. Ser. B. Biol. Sci.* **1967**, *167*, 365.
(16) Rupley, J. A.; Butler, L.; Gerring, M.; Hartdegen, F. J.; Pecoraro, R. *Proc. Natl. Acad. Sci. U.S.A.* **1967**, *57*, 1088.
(17) Banerjee, S. K.; Pogolotti, A.; Rupley, J. A. *J. Biol. Chem.* **1975**, *250*, 8260.
(18) Norton, R. S.; Allerhand, A. *J. Biol. Chem.* **1977**, *252*, 1795.
(19) Arakawa, T.; Bhat, R.; Timasheff, S. N. *Biochemistry* **1990**, *29*, 1914.
(20) Collins, K. D. *Biophys. J.* **1997**, *72*, 65.
(21) Judge, R. A.; Forsythe, E. L.; Pusey, M. L. *Biotechnol. Bioeng.* **1998**, *59*, 776.
(22) Sophianopoulos, A. J.; Van Holde, K. E. *J. Biol. Chem.* **1964**, *239*, 2516.
(23) Koppel, D. E. *J. Chem. Phys.* **1972**, *57*, 4814.
(24) Provencher, S. W. *Comput. Phys. Commun.* **1982**, *27*, 213.
(25) Provencher, S. W. *Comput. Phys. Commun.* **1982**, *27*, 229.
(26) Azuma, T.; Tsukamoto, K.; Sunagawa, I. *J. Crystal Growth* **1989**, *98*, 371.
(27) Mikol, V.; Hirsch, E.; Giegé, R. *J. Mol. Biol.* **1990**, *213*, 187.
(28) Nicoli, D. F.; Benedek, G. B. *Biopolymers* **1976**, *15*, 2421.
(29) Muschol, M.; Rosenberger, F. *J. Chem. Phys.* **1995**, *103*, 10424.
(30) Skouri, M.; Delsanti, M.; Munch, J. P.; Lorber, B.; Giegé, R. *FEBS Lett.* **1991**, *259*, 84.
(31) Arakawa, T.; Timasheff, S. N. *Biochemistry* **1982**, *21*, 6545.
(32) Melander, W.; Horvath, C. *Arch. Biochem. Biophys.* **1977**, *183*, 200.
(33) Pusey, P. N.; Tough, R. J. A. *Dynamic Light Scattering: Applications of Photon Correlation Spectroscopy*, 1st ed.; Plenum: New York, 1985; Chapter 4.
(34) Batchelor, G. K. *J. Fluid Mech.* **1976**, *74*, 1.
(35) Batchelor, G. K. *J. Fluid Mech.* **1983**, *131*, 155.
(36) Felderhof, B. U. *J. Phys. A: Math. Gen.* **1978**, *11*, 929.
(37) Phillies, G. D. J. *J. Phys. Chem.* **1995**, *99*, 4265.
(38) Phillies, G. C. J.; Hunt, R. H.; Strang, K.; Sushkin, N. *Langmuir* **1995**, *11*, 3408.
(39) Broide, M. L.; Tominc, T. M.; Saxowsky, M. D. *Phys. Rev. E* **1996**, *53*, 6325.
(40) Piazza, R. *J. Crystal Growth* **1999**, *196*, 415.
(41) Retailleau, P.; Ries-Kautt, M.; Ducruix, A.; Belloni, L.; Candau, S. J.; Munch, J. P. *Europhys. Lett.* **1999**, *46*, 154.
(42) Rosenbaum, D. F.; Kulkarni, A.; Ramakrishnan, S.; Zukoski, C. F. *J. Chem. Phys.* **1999**, *111*, 9882.
(43) Leikin, S.; Parsegian, V. A.; Rau, D. D.; Rand, R. P. *Annu. Rev. Phys. Chem.* **1993**, *44*, 369.
(44) Israelachvili, J.; Wennerstrom, H. *Nature* **1996**, *379*, 219.